Evolution of the Interfacial Area in Dendritic Solidification

H. Neumann-Heyme[1], K. Eckert[1,2] and C. Beckermann[3]

[1] Helmholtz-Zentrum Dresden-Rossendorf (HZDR), 01314 Dresden, Germany
[2] Institute of Process Engineering, Technische Universität Dresden, 01062 Dresden, Germany
[3] Department of Mechanical and Industrial Engrg., University of Iowa, Iowa City, IA 52242, USA

Abstract

The specific area of the solid-liquid interface is an important integral measure for the morphological evolution during solidification. It represents not only the inverse of a characteristic length scale of the microstructure, but it is also a key ingredient in volume-averaged models of alloy solidification. Analytical descriptions exist for either pure coarsening or pure growth processes. However, all alloy solidification processes involve concurrent growth and coarsening. In the present study, the kinetics of the solid-liquid interface of a dendrite are studied using a 3D phase-field model. The simulation results are combined with data from recent synchrotron tomography experiments to study the influence of the cooling rate and alloy composition on the evolution of the interfacial area. A general relation for the specific interfacial area of dendrites is presented that is valid over the entire range of cooling rates, including isothermal coarsening.

Keywords: Dendritic Solidification, Interfacial Area, Phase-Field Simulation

1. Introduction

A key aspect in modelling alloy solidification is the evolution of the shape of the solid-liquid interface. The specific area of the solid-liquid interface S_s, is an integral measure that describes the overall morphology [1, 2]. It is defined as the area of the interface A per volume of the enclosed solid phase V_s

$$S_s = A/V_s \tag{1}$$

The inverse of the specific interface area can be considered a characteristic length scale of the microstructure. The interfacial area density or concentration S_v, on the other hand, is defined as the ratio of the interface area to the sample volume V containing both solid and liquid phases,

$$S_V = A/V = g_s S_s \tag{2}$$

where $g_s = V_s/V$ is the solid volume fraction. Either quantity is a key ingredient in volume-averaged (macroscopic) models of alloy solidification and is needed, for example, in the modelling of microsegregation and melt flow in the semi-solid mush [3].

In the present study, phase-field simulations of dendritic growth are used to study the variation of the specific interface area with solid fraction and time. A general interface evolution equation is proposed that fits the simulation data for a large range of cooling rates, including isothermal coarsening. Then, data from previously performed high-speed synchrotron tomography solidification experiments [4-6] are used to validate the general interface evolution equation. Finally, the present results in the limit of isothermal coarsening are compared to previous experiments and theories.

2. Phase-field simulations

Three-dimensional phase-field simulations of columnar dendritic alloy solidification were conducted using the well-established phase-field model for directional solidification of a dilute binary alloy of Echebarria et al. [7], which assumes that the temperature field is given by a moving temperature gradient. The model is extended to include finite-rate solute diffusion in the solid [8]. Details of the numerical implementation can be found in Refs. [9, 10].

The material data used in the simulations are representative of an Al-Cu alloy and are given by an initial alloy solute concentration C_0 = 6 wt.%, liquidus slope m = -2.6 K/wt.%, melting point of pure aluminium T_m = 660 °C, partition coefficient k = 0.14, solute mass diffusivities in the liquid D_l = 3000 μm²/s and solid D_s = 0.3 μm²/s, respectively, Gibbs-Thomson coefficient Γ = 0.24 μmK, and surface energy anisotropy coefficient ε = 0.02.

2.1 Simulation results

A base case simulation was conducted that corresponds to a pulling speed of V_p = 300 μm/s and a temperature gradient of G = 200 K/cm, resulting in a cooling rate of $\dot{T}_0$ = -6 K/s.

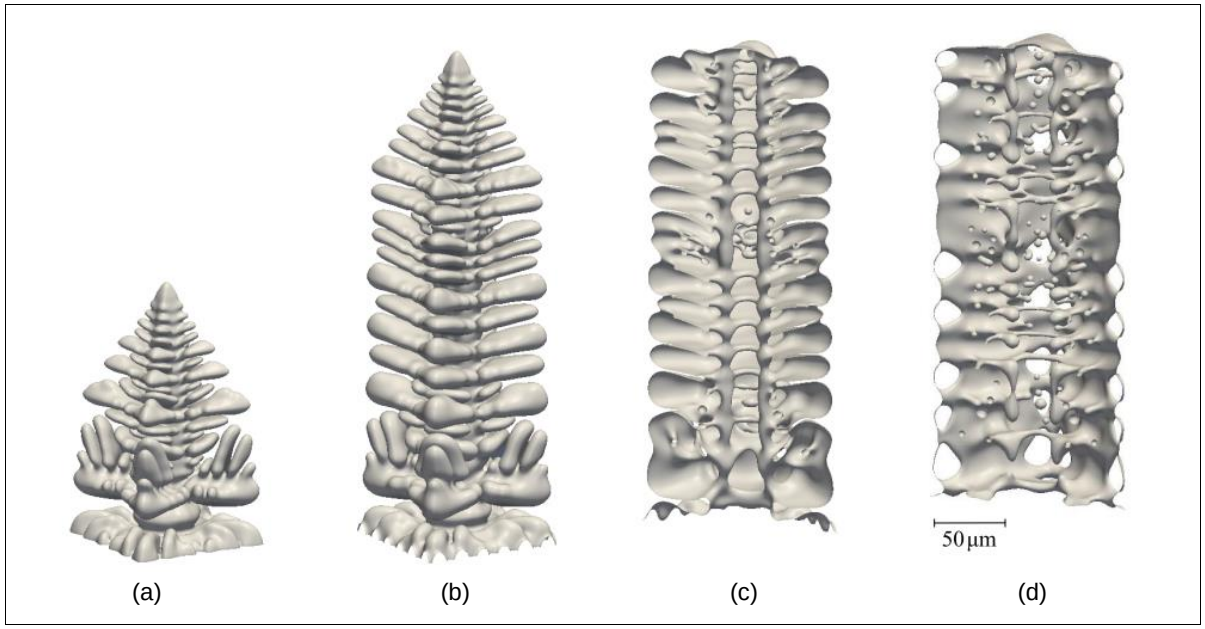

Figure 1: Evolution of the dendrite geometry for the base case simulation: full view of the growing dendrite at 0.5 s (a) and 1 s (b); cutaway view of half of the dendrite at 2.5 s (c) and 7 s (d).

Figure 1 shows snapshots of the computed dendrite at four different times. During the first second (Figures 1a and 1b) the primary dendrite tip translates the entire length of the simulation domain. Numerous secondary dendrite branches develop behind the primary tip, causing a rapid increase in the interface area. At later times (Figures 1c and 1d), the solid volume fraction continues to increase and coalescence of sidebranches can be observed. The impingement of interfaces eventually leads to the development of liquid channels and pockets inside the solid structure (Figure 1d).

The interface area and the solid volume of the dendrite shown in Figure 1 were measured over a suitably sized sample volume located at mid-height [9]. The calculated variation of the interfacial area density with solid volume fraction is shown in Figure 2a. For the base case simulation, the interfacial area density first increases with solid fraction, which can be attributed to the formation and growth of the dendrite side arms. It reaches a maximum at a solid fraction of about 0.6 and then Figure 2a also contains results for three other simulations where the cooling rate was abruptly changed at a solid volume fraction of 0.3. Cooling rates of 0.5, 0.1 and 0 times the base case cooling rate were examined, with the cooling rate of 0 representing isothermal coarsening at a constant solid fraction. It can be seen that the lower cooling rates result in smaller interfacial area densities, with the onset of interface coalescence shifted to lower solid fractions.

2.2 General interface evolution equation

A general evolution equation for the specific interface area is proposed here as

$$S_s^{-1} = (1-g_s)^{-r}(S_{s0}^{-3} + K_0 t)^{1/3} \qquad (3)$$

where r, S_{s0} and K_0 are fitting parameters. The first term on the right-hand-side of Equation (3) accounts for diffusional interactions and interface coalescence, which becomes increasingly important when the solid volume fraction approaches unity. The second term has the same form as a classical surface energy driven coarsening law [1, 2]. The exponent of 1/3 has been found to be valid not only for pure coarsening, but also for concurrent growth and coarsening [11, 12]. Figure 2b shows that Equation (3) does provide a reasonable fit to the present simulation results for all cooling rates. The resulting values of the three fitting parameters are provided in the figure. It is interesting to note that the value of $(S_{s0})^{-1}$ is close to the primary dendrite tip radius, which was measured to be equal to 2.7 μm. Figure 2a shows that the present fit also captures the overall behaviour of the variation of the interfacial area density with solid fraction.

3. Experimental validation

The general interface evolution equation, Equation (3), is validated using data from four high-speed synchrotron tomography experiments [4-6]. In these experiments, the interface area and solid volume in a representative volume element were measured in real time during solidification. Table 1 lists the main parameters of the experiments and Figure 3 shows the fit of the experimental data to Equation (3). In the figure, the solid fraction and time dependent terms in Equation (3) are separated as

$$\eta = \left[S_s^{-1} S_{s0} (1-g_s)^r \right]^3 - 1 \quad \text{and} \quad \xi = K_0 t S_{s0}^3 \qquad (4)$$

It can be seen that all data fall close to the line $\eta = \xi$, which indicates perfect agreement with Equation (3). The fitting results in an exponent r = 0.25 (for all experiments), as opposed to r = 0.4 for the phase-field simulations. This difference may be explained by the highly regular arrangement of the dendrites in the simulations leading to stronger interface coalescence. The values of the rate constant K_0 resulting from fitting each of the experiments are listed in Table 1. Note that the rate constants for the

two Mg-15wt.%Sn experiments (C and D) are close to each other, indicating that, as in the simulations, K_0 is independent of the cooling rate.

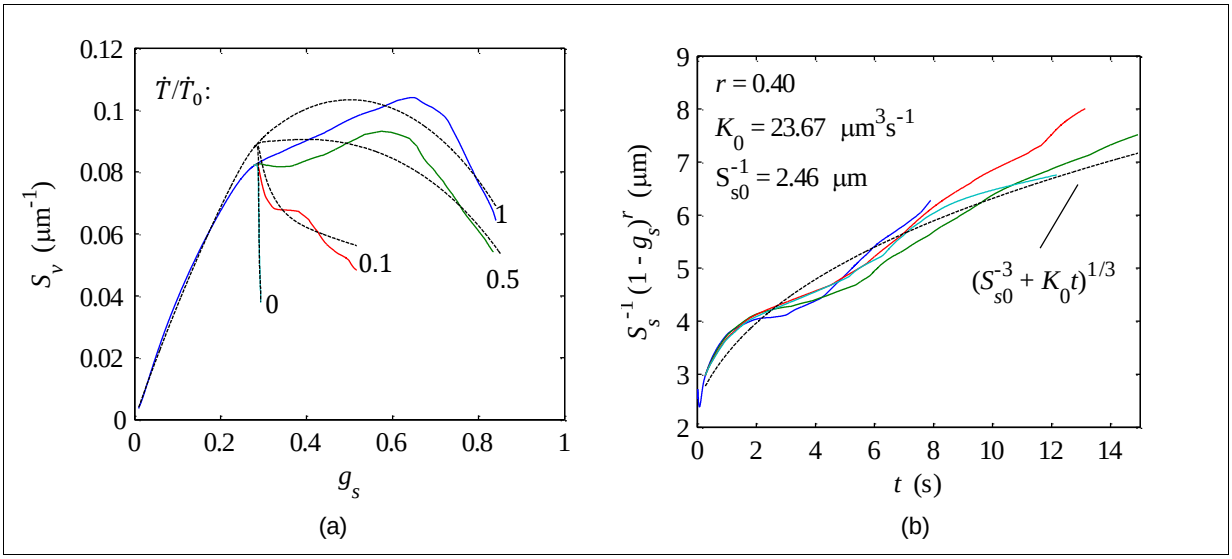

Figure 2: Computed variation of the interfacial area density and inverse specific interface area for four different cooling rates. The dashed lines are the fit given by the general interface evolution equation, Equation (3).

Table 1: Experimental parameters and values of the rate constant obtained from the fits of the data to Equation (3).

Exp.	Ref.	Alloy	$\dot{T}$ (K/min)	K_0 (μm^3/s)
A	[4]	Al-10wt.%Cu	-3	9.58
B	[5]	Al-24wt.%Cu	-2	3.05
C	[6]	Mg-15wt.%Sn	-3	26.28
D	[6]	Mg-15wt.%Sn	-12	24.53
Simulations:		Al-6wt.%Cu	-360 to 0	23.67

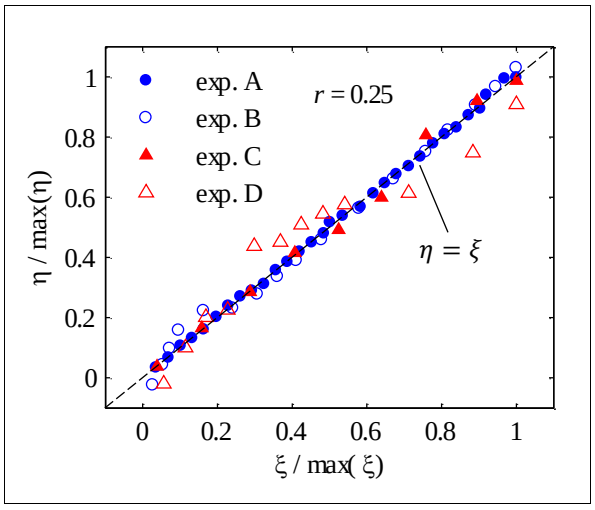

Figure 3: Fit of the synchrotron tomography data to Equation (3).

4. Isothermal coarsening limit

Comparing Equation (3) to classical surface energy driven isothermal coarsening (ripening) laws [12], a coarsening rate constant K can be defined as

$$K = K_0(1-g_s)^{-3r} \quad (5)$$

Hence, K_0 is nothing but an isothermal coarsening rate constant in the limit of vanishing solid fraction.

Theories of isothermal coarsening [12] show that K_0 can be expressed in terms of alloy properties as

$$K_0 = aD_l d_0 \quad (6)$$

where d_0 is the chemical capillary length defined as $d_0 = \Gamma/(|m|C_0(1-k))$ and a is an unknown constant. The product $D_l d_0$ for the Al-Cu experiments in Table 1 (A and B) is evaluated using m = -3.3 and -4.3 K/wt.% as well as k = 0.13 and 0.16 for C_0 = 10 and 24 wt.%, respectively. The different values for m and k reflect the non-linear nature of the Al-Cu phase diagram. The Gibbs-Thomson coefficient and the solute diffusivity are taken as Γ = 0.24 μmK and D_l = 2400 μm^2/s, respectively, for both alloys. For the phase-field simulations with C_0 = 6 wt.%, the product $D_l d_0$ is evaluated using the Al-Cu properties listed in Section 2. Figure 4 shows that K_0 can indeed be predicted by Equation (6) with a = 0.45. The Mg-Sn experiments of Table 1 are not included in the figure due to uncertainties in the properties.

The variation of the isothermal coarsening rate constant K with solid fraction, as provided by Equation (5), is validated in Figure 5 using experimental data from three different pure coarsening studies involving four different alloys [13-15]. It can be seen that Equation (5) with r = 0.25, as determined in the previous section from the synchrotron tomography solidification experiments,

fits the pure coarsening data for the rate constant very well. Even the value of r = 0.4, as determined from the phase-field simulations, provides a reasonable fit.

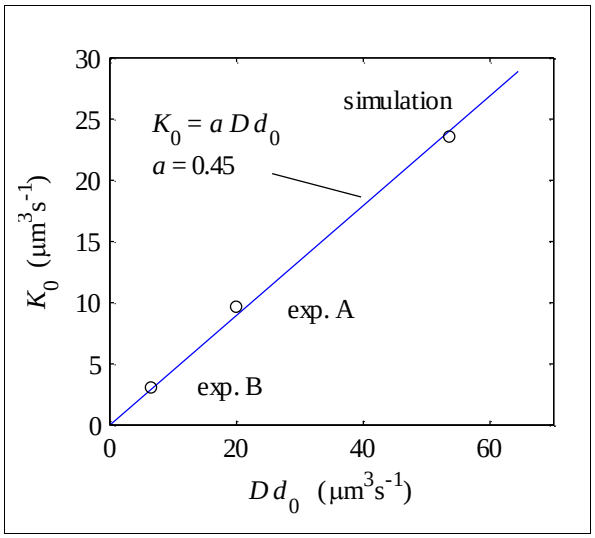

Figure 4: Variation of the isothermal coarsening rate constant in the limit of vanishing solid fraction with properties for the Al-Cu alloys of Table 1.

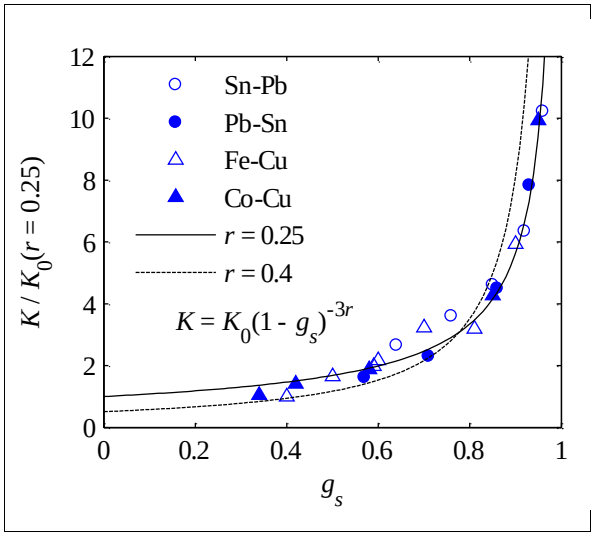

Figure 5: Comparison of the solid fraction dependency of the coarsening rate constant with experimental data from isothermal coarsening experiments [13-15].

4. Conclusions

A general evolution equation for the specific interface area during dendritic alloy solidification, Equation (3), has been developed using data from both phase-field simulations and synchrotron tomography measurements. This equation contains both the solid volume fraction and time as independent variables. It is shown to be valid for a large range of cooling rates, including isothermal coarsening, and arbitrary (binary) alloy compositions.

The present evolution equation for the specific interface area contains three fitting parameters: r, S_{s0} and K_0. Experimental data for both solidification and isothermal coarsening show that the exponent r is equal to 0.25; however, for the highly regular dendrite arrangement of the phase-field simulations, r = 0.4 provides a better fit. The inverse of the initial specific interface area, S_{s0}, appears to be close to the primary dendrite tip radius, which in turn can be predicted using classical theories [16]; however, additional study is necessary to confirm this finding. The rate constant is given by $K_0 = 0.45\, D_l d_0$.

Future research should be aimed at extending the interface evolution equation to multiple phases, including eutectic and peritectic solidification, and multi-component alloys.

Acknowledgements

This work was financially supported by the Helmholtz Association (LIMTECH) and NASA (NNX14AD69G). We thank the supercomputing center in Jülich (HDR08) for providing computing time.

References

1. S. Marsh *et al.*, *Metall. Mater. Trans. A*, 1996, **27**: 557.
2. R. Mendoza *et al.*, *Metall. Mater. Trans. A*, 2003, **34**: 481.
3. J. Ni *et al.*, *Metall. Trans. B*, 1991, **22**: 349.
4. N. Limodin *et al.*, *Acta Mater.*, 2009, **57**:2300.
5. J.W. Gibbs *et al.*, *Sci. Rep.*, 2015, **5**: 11824.
6. S. Shuai *et al.*, *Acta Mater.*, 2016, **118**: 260.
7. B. Echebarria *et al.*, *Phys. Rev. E*, 2004, **70**: 061604.
8. M. Ohno *et al.*, *Phys. Rev. E*, 2009, **79**: 31603.
9. H. Neumann-Heyme *et al.*, *IOP Conf. Series: Mater. Sci. Eng.*, 2015, **84**: 012072.
10. H. Neumann-Heyme *et al.*, *Phys. Rev. E*, 2015, **92**: 060401(R).
11. L. Ratke *et al.*, *Acta Mater.*, 2001, **49**: 4041.
12. L. Ratke *et al.*, *Growth and Coarsening*, Springer, Heidelberg, Germany, 2002.
13. S.C. Hardy *et al.*, *Metall. Trans. A*, 1988, **19**: 2713.
14. A.N. Niemi *et al.*, *J. Mater. Sci.*, 1981, **16**: 226.
15. S. Kang *et al.*, *Metall. Trans. A*, 1982, **13**: 1405.
16. J.A. Dantzig *et al.*, *Solidification*, EPFL Press, Lausanne, Switzerland, 2009.

SP17

Solidification Processing 2017

Proceedings of the
6th Decennial
International Conference on
Solidification Processing

25 - 28 July 2017
Beaumont Estate
Old Windsor, UK

Edited by Z. Fan

BCAST

Solidification Processing 2017: Proceedings of the
6th Decennial International Conference on Solidification Processing
edited by Professor Zhongyun Fan.

First published in Great Britain in 2017
by BCAST, Brunel University London.

Typeset and printed in the UK by SS Media, Hertfordshire.

ISBN – 978-1-908549-29-7
6th Decennial International Conference on Solidification Processing
c/o Brunel Centre for Advanced Solidification Technology
Brunel University London
Uxbridge
Middlesex
UB8 3PH, UK
www.brunel.ac.uk/bcast